Efficient Catalytic Activity of Transition Metal Ions in Vilsmeier–Haack Reactions with Acetophenones

ARTICLE *in* INTERNATIONAL JOURNAL OF CHEMICAL KINETICS · AUGUST 2013

Impact Factor: 1.52 · DOI: 10.1002/kin.20807

3 AUTHORS, INCLUDING:

F. Aneesa

Muffakham Jah College of Engineering and …

4 PUBLICATIONS **0** CITATIONS

SEE PROFILE

Chinna Rajanna Kamatala

Osmania University

118 PUBLICATIONS **500** CITATIONS

SEE PROFILE

Efficient Catalytic Activity of Transition Metal Ions in Vilsmeier–Haack Reactions with Acetophenones

F. ANEESA,[1] K. C. RAJANNA,[2] M. VENKATESWARLU,[2] K. RAJENDAR REDDY,[2] Y. ARUN KUMAR[1]

[1]*Department of Chemistry, M. J. C. E. T., Hyderabad, India*

[2]*Department of Chemistry, Osmania University, Hyderabad* 500 007, *India*

Received 24 January 2013; revised 9 May 2013; 31 May 2013; accepted 2 June 2013

DOI 10.1002/kin.20807
Published online 3 August 2013 in Wiley Online Library (wileyonlinelibrary.com).

ABSTRACT: Vilsmeier–Haack (VH) formylation reactions with acetophenones are sluggish in acetonitrile medium even at elevated temperatures. However, millimolar concentrations of transition metal ions such as Cu(II), Ni(II), Co(II), and Cd(II) were found to exhibit efficient catalytic activity in Vilsmeier–Haack Reactions with acetophenones. Reactions are accelerated remarkably in the presence of transition metal ions. The VH reactions followed second order kinetics and afforded acetyl derivatives under kinetic conditions also irrespective of the nature of oxychloride ($POCl_3$ or $SOCl_2$) used for the preparation of VH reagent along with DMF. On the basis of UV–vis spectroscopic studies and kinetic observations, participation of a ternary precursor [M(II) S (VHR)] in the rate-limiting step has been proposed to explain the mechanism of the metal ion–catalyzed VH reaction. © 2013 Wiley Periodicals, Inc. Int J Chem Kinet 45: 721–733, 2013

INTRODUCTION

Chromone derivatives have been the subject of considerable pharmaceutical and chemical interest in the recent past, because of their broad spectrum of biological activities such as antifungal, antiviral, antimicrobial, antiallergenic, antitubulin, and antitumor activity [1–5]. Besides, many flavonoids are based on the chromone structure and have been shown to exhibit therapeutically interesting biological activities [5]. More specifically, 3-formylchromones have been extensively used as versatile building blocks for the synthesis of a large number of heterocyclic systems [6–10]. Inspired by the versatility of the Vilsmeier–Haack (VH) reagent, there has been an upsurge in the past several years to explore its use for formylation, acetylation, cyclization, benzylation, bromination, nitration, and sulfonation reactions [8–17]. One-pot synthesis of 3-formylchromones has also been achieved smoothly from *o*-hydroxy acetophenones under VH conditions from our laboratories and elsewhere [18–22]. However, an insight into the reaction times of VH reactions for 3-formylchromones indicates that the reactions are very slow under conventional conditions [18–22]. This

Correspondence to: K. C. Rajanna; e-mail: kcrajannaou@yahoo.com.

Supporting Information is available in the online issue at www.wileyonlinelibrary.com.

prompted the author to use an ecofriendly additive as a catalyst to enhance the synthesis. Transition metals and their compounds function as catalysts either because of their ability to change the oxidation state or, in the case of the metals, to adsorb other substances onto their surface and activate them in the process. Transition metals are good metal catalysts because they easily lend and take electrons from other molecules [23,24]. Recently, Hegedus has published a review on the use of transition metals as catalysts in organic synthesis. It offered a fairly comprehensive coverage of the literature, with extensive citations, unusual and significant transformations in organic synthesis [25]. The present study is one such exercise in which transition metal ions such as Cu(II), Ni(II), Co(II), and Cd(II) are used as catalysts to explore the synthesis, kinetics, and mechanism of VH reactions with acetophenones and hydroxy acetophenones.

EXPERIMENTAL

VH Reagents

Flasks containing DMF dissolved in a suitable solvent (generally DCE, or MeCN) along with $SOCl_2$ and $POCl_3$ were cooled and thermally equilibrated for about 30 min at –5°C by keeping in a benzene trough chilled from outside with ice and NaCl. Requisite amounts of solvent and amide were transferred into a 100-mL flask, and $POCl_3$ or $SOCl_2$ was added dropwise at –5°C with constant stirring. The resultant reagent mixture was kept aside for about 1 h to ensure complete formation of the VH adduct. Its concentration was checked by acid–base titrations at Bromocresol Green end point according to literature reports [7–9].

Kinetics of the Study

It is also proposed to study the kinetics of the reaction as reported in the papers published from our laboratories [7,8]. Aliquots of the reaction mixture were quenched in hot water at different intervals of time and kept a side for at least **2** h to allow the hydrolysis of the unreacted [VH adduct]. Upon hydrolysis, the VH adduct liberates a mixture of phosphoric and hydrochloric acids. The acid content thus liberated is titrated against standard NaOH using Bromocresol Green as an indicator.

Product Analysis under Kinetic Conditions

After completing the kinetic study of the reaction, excess (remaining part) of the reaction mixture was refluxed further for 4–5 h and left aside overnight. The solution was poured into ice-cold water with vigorous stirring and kept aside for about 2 h. The resultant solution was neutralized by sodium hydrogen carbonate. The organic phase was extracted with DCE and dried $MgSO_4$, and the solvent evaporated. Products of the reaction were isolated under kinetic conditions and found to be acetyl derivatives of the substrates. The products were characterized by ^1H NMR and mass spectra with authentic samples and found to be satisfactory. It is interesting to note that orthohydroxy acetophenone (OHAP) underwent cyclization followed by formylation and afforded 3-formyl chromone and 2,5–dihydroxy acetophenone (DHAP) afforded 3-formyl-6-hydroxy-chromone without affecting the second hydroxyl group as described in our earlier work [16,17], while acetophenone and 4-nitroacetophenone did not undergo cyclization but afforded the corresponding formyl derivatives (Table I):

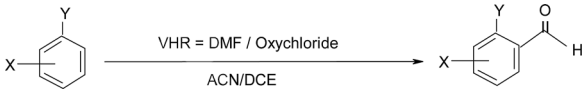

where VHR = DMF + ($SOCl_2$ or $POCl_3$), Y = $-COCH_3$, and X = electron donating or electron-withdrawing groups

RESULTS AND DISCUSSION

Kinetic Features of the Present Study

The kinetic and mechanistic features of transition metal ion–mediated VH reactions with hydroxyacetophenones are by and large similar to those observed in earlier studies. Reaction kinetics indicated first order in [VHR] as could be seen from the linear plots of ln V_t versus time (Fig. 1), when $[\text{substrate}]_0 \gg [\text{VHR}]_0$. However, under the conditions $[\text{VHR}]_0 = [\text{substrate}]_0$, plots of $[1/(a-x)]$ or $[1/V_t]$ versus time were linear with a positive slope and an intercept on the ordinate, indicating that VH reaction follows over all second-order kinetics. Certain second-order plots are presented in Fig. 2. Rate constant data pertaining to first-order and second-order kinetics are presented in Tables II and III.

Effect of [M(II)]: Reactions underwent significant rate accelerations in the presence of transition metal ions such as Cu(II), Ni(II), Co(II), and Cd(II), which can be seen from the data presented in Table III.

Reactive Species and Mechanistic Features

The kinetic features observed in the present work are by and large similar to those reported earlier from our laboratory using DMF/$POCl_3$ as a VH reagent [14,15]. A perusal of the publications from our laboratory [14,15] coupled with other literature reports [2–5] suggests that

Table I Metal Ion–Catalyzed VH Formylation Reactions of Certain Acetophenones VHR = (Oxychloride + DMF) = 1:1, [M(II)] = 1.0 m mol

VHR	Substrate	Product	Native		Cu(II)		Ni(II)		Co(II)		Cd(II)	
			RT (h)	Percentage Yield	RT (h)	Percentage Yield	RT (h)	Percentage Yield	RT (h)	Percentage Yield	RT (h)	Percentage Yield
$DMF/POCl_3$	Acetophenone	β-Chlorocinnamaldehyde	18	40	8	74	12	74	8	76	8	75
	Orthohydroxy acetophenone	3-Formylchromone	18	42	6	83	8	83	6	86	6	80
	2,5–Dihydroxy acetophenone	3-Formyl 6-hydroxy-chromone	18	40	12	75	14	75	12	78	12	75
	4-Nitroacetophenone	4-Nitrocinnamaldehyde	24	30	15	58	18	58	15	62	16	62
$DMF/SOCl_2$	Acetophenone	β-Chlorocinnamaldehyde	18	40	8	74	12	74	8	76	8	75
	Orthohydroxy acetophenone	3-Formylchromone	18	42	6	83	8	83	6	86	6	80
	2,5–Dihydroxy acetophenone	3-Formyl–6-hydroxy-chromone	18	40	12	75	14	75	12	78	12	75
	4-Nitroacetophenone	4-Nitrocinnamaldehyde	24	30	15	58	18	58	15	62	16	62

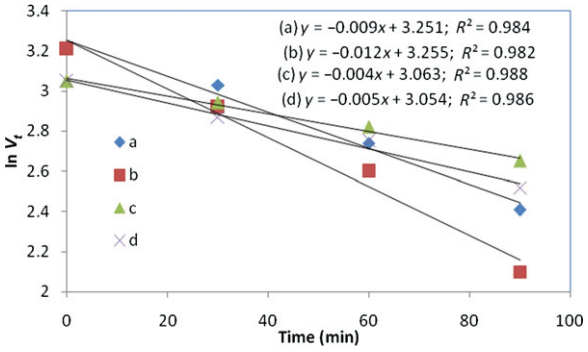

Figure 1 First-order kinetic plots for VH formylation of orthohydroxy acetophenone at 333 K and MeCN solvent. (a) Uncatalyzed reaction, [Sub] = 0.09 mol/dm^3; [VHR] ($POCl_3$+DMF) = 0.005 mol/dm^3. (b) Cu(II)-catalyzed VH reaction using ($POCl_3$+DMF). (c) Uncatalyzed VH formylation of orthohydroxy acetophenone using ($SOCl_2$+DMF). (d) Cu(II)-catalyzed formylation using ($SOCl_2$+DMF).

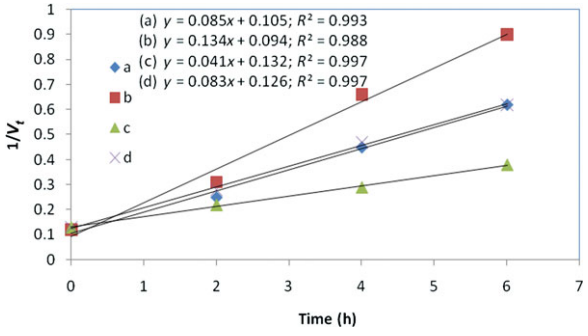

Figure 2 Second-order kinetic plots for VH formylation of orthohydroxy acetophenone at 333 K and MeCN solvent. (a) Uncatalyzed reaction using ($POCl_3$+DMF) as VH reagent. (b) Cu(II)-catalyzed reaction using ($POCl_3$+DMF) as VH reagent. (c) Uncatalyzed VH formylation of orthohydroxy acetophenone using ($SOCl_2$+DMF). (d) Cu(II)-catalyzed formylation using ($SOCl_2$+DMF).

the VH reagent, in solution, is present in a number of covalent, ion-pair, and cationic forms [DMF/$SOCl_2$] reagent in the lines of [DMF/$POCl_3$] reagent. Isolated products of the reaction are also similar to those of earlier work. On the basis of these similar experimental observations, it is reasonable to consider a similar type of reactive species in both (DMF/$POCl_3$) and (DMF/$SOCl_2$) systems. Accordingly, species could be written as (I) to (IV) in the (DMF/$POCl_3$) system and (V) to (VIII) in the (DMF/$SOCl_2$) system:

$$[(CH_3)_2\,N{=}CHCl]^+\,[OPOCl_2]^- \quad (I)$$

$$[(CH_3)_2\,N{=}CH-OPOCl_2]^+\,Cl^- \quad (II)$$

Table II VH Formylation First-Order Reactions with Acetophenones [Subs] = 0.09 mol/dm^3; [VHR] = 0.005 mol/dm^3; M(II) = 0.001 mol/dm^3

		First-Order Rate Constant (10^5 k' /s)				
VHR	Substrate	Native	Cu(II)	Ni(II)	Co(II)	Cd(II)
DMF/$POCl_3$	Acetophenone	3.33	5.00	5.00	5.0	5.0
	Orthohydroxy acetophenone	15.0	20.0	18.0	18.0	17.0
	2,5-Dihydroxyacetophenone	13.3	20.0	18.0	18.0	15.0
	4-Nitroacetophenone	11.6	15.0	13.0	13.0	12.0
DMF/$SOCl_2$	Acetophenone	5.00	6.67	6.67	6.67	6.67
	Orthohydroxy acetophenone	6.60	8.33	8.33	8.33	8.33
	2,5-Dihydroxyacetophenone	3.33	3.33	3.33	3.33	3.33
	4-Nitroacetophenone	3.33	5.00	5.00	5.00	5.00

Table III Temperature-Dependent Second-Order Rate Constants and Activation Parameters for VH Formylation Reactions with Acetophenones in MeCN Medium

			Second-Order Rate Constant ($\times 10^4$ k dm^3/mol/s)				
System	Substrate	Temperature (K)	Uncatalyzed	Cu(II)	Ni(II)	Co(II)	Cd(II)
DMF/$POCl_3$	Acetophenone	313	6.16	11.3	10.8	10.1	7.20
		323	15.7	28.1	25.4	25.7	20.1
		333	38.6	59.4	53.46	60.48	47.6
	OHAP	313	7.28	14.6	12.96	10.64	10.0
		323	19.0	27.5	27.5	25.8	26.3
		333	47.6	72.3	59.9	63.3	61.0
	2,5-Dihydroxyacetophenone	313	7.28	13.5	11.9	11.2	10.1
		323	20.7	39.9	34.0	33.0	28.5
		333	55.4	103.0	89.1	82.3	73.3
	p-Nitroacetophenone	313	6.72	9.72	8.64	8.40	7.20
		323	17.3	22.7	21.1	20.7	19.0
		333	45.9	74.5	66.9	63.3	58.8
DMF/$SOCl_2$	Acetophenone	313	5.60	10.08	9.50	8.40	7.30
		323	14.0	25.76	24.64	21.84	17.9
		333	33.0	60.5	57.1	57.1	43.7
	OHAP	313	3.36	6.70	6.16	5.04	4.50
		323	8.96	17.9	16.8	13.4	11.8
		333	22.9	46.4	42.0	36.9	31.9
	2,5-Dihydroxyacetophenone	313	2.24	4.40	3.92	3.36	2.20
		323	6.16	12.3	10.6	8.90	7.30
		333	16.8	38.6	27.4	21.8	20.2
	p-Nitroacetophenone	313	3.36	8.40	8.40	7.84	3.40
		323	11.7	22.4	20.7	20.1	13.4
		333	33.0	51.5	48.1	47.6	41.4

$$[(CH_3)_2\ N{=}CHClOPOCl_2]^+ \quad \text{(III)}$$

$$[(CH_3)_2\ H_2N{=}CHCl]^+ \quad \text{(IV)}$$

$$[(CH_3)_2\ N{=}CHCl]^+\ [OSOCl]^- \quad \text{(V)}$$

$$[(CH_3)_2\ N{=}CH-OSOCl]^+\ Cl \quad \text{(VI)}$$

$$[(CH_3)_2\ N{=}CHClOSOCl]^+ \quad \text{(VII)}$$

$$[(CH_3)_2\ H_2N{=}CHCl]^+ \quad \text{(VIII)}$$

In our earlier publications on VH reactions [16–18], we reported second-order kinetics with first order in [substrate] and first order in [VH] reagent, and the reaction rates were faster at a low dielectric dichloroethane (DCE) solvent as compared to a high dielectric acetonitrile (MeCN) medium with the trend: DEC > MeCN. On the basis of these observations, the possibility of a change in the reactive species was suggested, passing from higher dielectric acetonitrile to low dielectric dichloroethane medium according to the

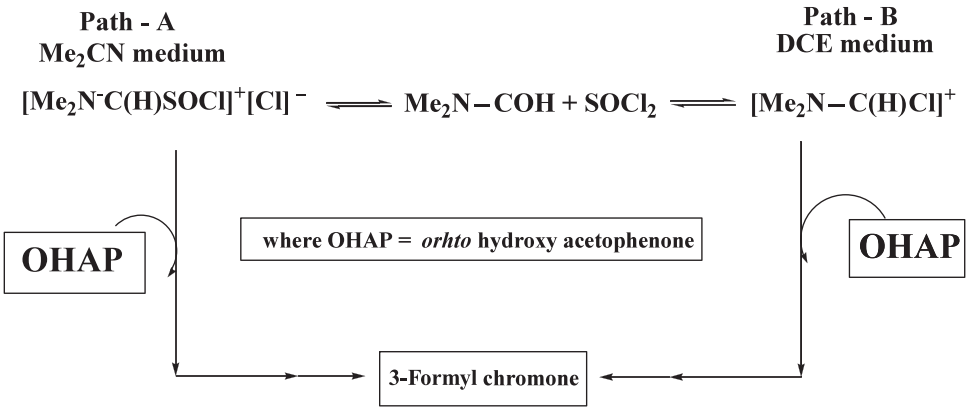

Scheme 1 Reaction mechanism for the uncatalyzed VH reaction with OHAP.

Ingold rule. Cationic $[(CH_3)_2\ H_2N = CHCl]^+$ species were suggested in DCE medium, whereas ion-pair species $[(CH_3)_2\ N = CHCl]^+\ [OPOCl_2]^-$/$[(CH_3)_2\ N = CHCl]^+\ [OSOCl]^-$ were considered in MeCN medium as shown in Scheme 1.

Products of the reaction were separated by TLC according to literature procedures. Products of the reaction were also analyzed by spectroscopy according to literature procedures. Acetyl derivatives have been found to be the products irrespective of the nature of the VH reagent used, as was depicted by similar IR spectra of the isolated product. For the above scheme, the rate law comes out as

$$\frac{-d[\text{Substrate}]}{dt} = k\ [\text{Substrate}]\ [\text{VH adduct}]$$

This rate-law explains second-order kinetics with a first-order dependence on [substrate] and also on [VH adduct], showing the consistency of the proposed mechanism. It is of interest to note that OHAP underwent cyclization followed by formylation to afford formyl chromone.

Mechanism of VH Reactions in Metal Ion–Catalyzed Reactions

The mechanistic path in metal ion–catalyzed VH reactions depends on several factors such as metal ion interactions with the substrate, VH reagent to give binary/ternary precursor(s) prior to the rate-limiting step. To ascertain the [M(II)-S], [M(II)-VHR], and [M(II)-S-VHR] interaction, spectrophotometric studies have been performed. As a typical case, Cu(II), Ni(II), and Co(II) interactions were studied with OHAP in the presence and absence of VHR. All the three metal ions indicated absorption bands in the visible region (electronic absorption spectra of Cu(II), Ni(II), and Co (II) indicated bands at 756, 490, and 512 nm, respectively). These bands underwent hypsochromic or bathochromic shifts in the presence of acetophenones with or without VHR as shown in Figs. 3–5 and Table IV. These observations indicate binary and ternary complex formation in the presence of VHR. In the presence of OHAP, Cu(II) and Ni(II) underwent a hypsochromic shift, whereas Co(II) indicated a bathochromic shift. These shifts establish the formation of binary complexes with OHAP. However, in the presence of VHR and OHAP, the metal ions underwent hypsochromic shifts, depicting the formation of ternary precursors prior to rate-limiting steps, as shown in Schemes 2 and 3. [M(II)-S] and [M(II)-VHR] binding constants were determined by using the Benesi–Hildebrand method [25] according to the following equilibria and relationships:

Metal Ion–Substrate Interactions.

$$\text{M(II)} + \text{S} \overset{K_1}{\rightleftharpoons} \text{M(II)S}$$

$$\Rightarrow \quad [\text{M(II)S}] = \frac{K_1[\text{M(II)}]C_S}{1 + K_1[\text{M(II)}]} \qquad (1)$$

To observe one-to-one binding between a single substrate (S) and metal ion (M) using UV–vis absorbance, the Benesi–Hildebrand method can be now employed. Using the Beer–Lambert law, the concentration of [M(II) S] can be rewritten as

$$A = \varepsilon\ [\text{M(II)S}]\ \ b\ \ (\text{where } b = \text{path length})$$

$$\Rightarrow [\text{M(II)S}] = A/\varepsilon\ b; \text{ and when } b = 1\,\text{cm}$$

$$\Rightarrow \quad [\text{M(II)S}] = A/\varepsilon$$

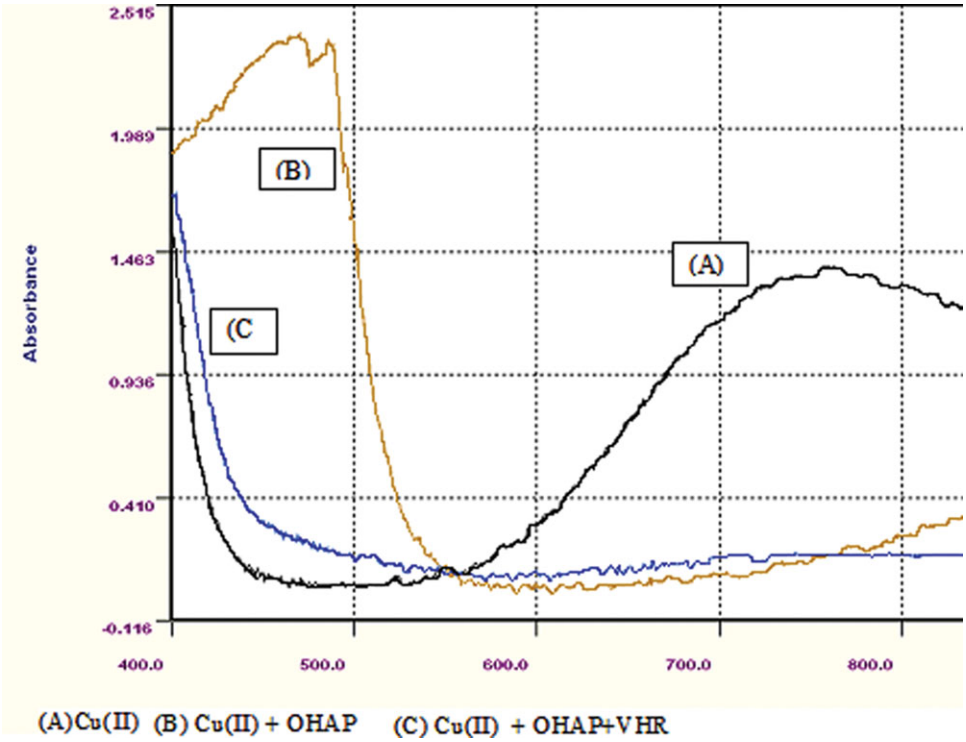

Figure 3 UV–vis spectra of Cu(II) with OHAP and VHR.

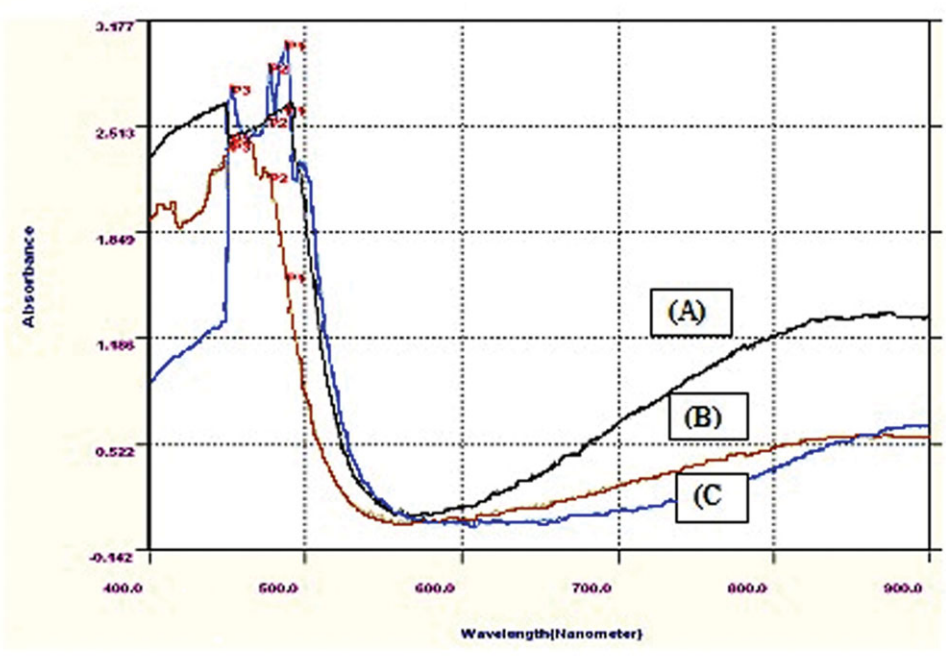

Figure 4 UV–vis spectra of Ni(II) with OHAP and VHR.

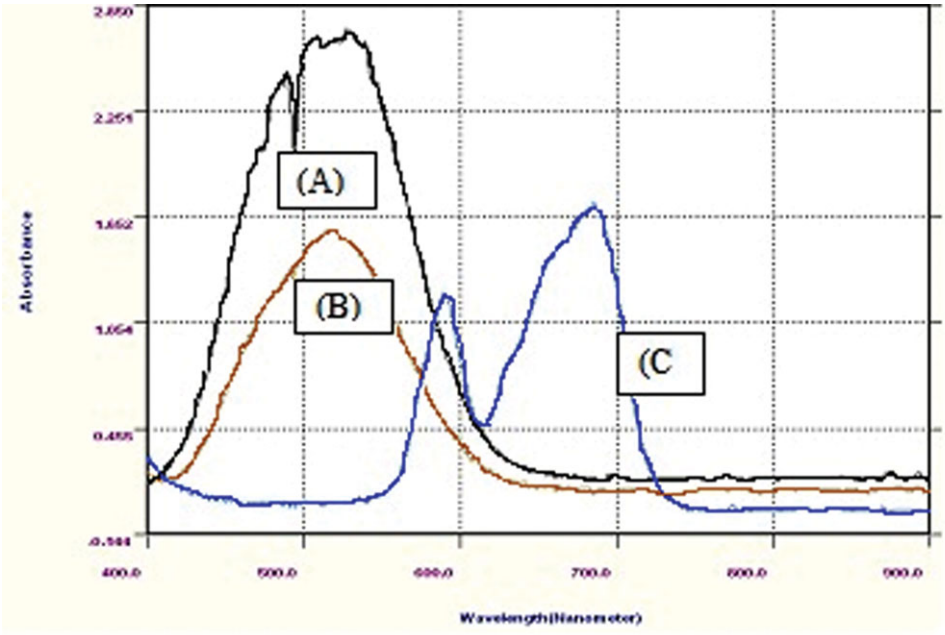

Figure 5 UV–vis spectra of Co(II) with OHAP and VHR.

Substituting for [M(II)S] in the binding isotherm equation (1), the equilibrium constant K can now be correlated to the change in absorbance due to the formation of the M(II)S complex:

$$\Rightarrow \frac{A}{\varepsilon} = [\mathrm{M(II)S}] = \frac{K_1\ [\mathrm{M\,(II)}]\ C_\mathrm{S}}{1 + K_1\ [\mathrm{M\,(II)}]}$$

Rearranging the above equation,

$$\Rightarrow \frac{A}{C_\mathrm{S}} = [\mathrm{M(II)S}] = \frac{\Delta\varepsilon K_1\ [\mathrm{M\,(II)}]}{1 + K_1\ [\mathrm{M\,(II)}]}$$

$$\Rightarrow \frac{C_\mathrm{S}}{A} = \frac{1}{\Delta\varepsilon K_1\ [\mathrm{M\,(II)}]} + \frac{1}{\Delta\varepsilon}$$

A double reciprocal plot can be made with (C_S /A) as a function of 1/[M(II)], and ε can be derived from the intercept, whereas K_1 can be calculated from the slope. Such reciprocal plots have been realized in this study (Fig. 6). The values of K_1 and ε are presented in Table IV.

Interaction of Metal Ion with the Substrate in the Presence of VHR. The model for ternary complex formation in micellar media is represented in the following equilibria:

$$\mathrm{M(II)} + \mathrm{S} \overset{K_1}{\rightleftharpoons} \mathrm{M(II)S}$$

$$\mathrm{M(II)S} + \mathrm{VHR} \overset{K_1}{\rightleftharpoons} [\mathrm{M(II)S - VHR}]$$

In the above scheme, M, S, and VHR represent metal ion, substrate, brominating reagent, whereas [M (II) S] and [M (II) S-VHR] refer to binary and ternary complexes formed due to the interaction of metal ion, substrate, and VHR, respectively:

$$[\mathrm{M(II)S - VHR}] = K_2\,[\mathrm{M(II)S}]\,[\mathrm{VHR}]$$

$$[\mathrm{M(II)S}] = K_1\,[\mathrm{M(II)}]\,[\mathrm{S}] \Rightarrow [\mathrm{S}]$$

$$= [\mathrm{M(II)S}]\big/K_1\,[\mathrm{M\,(II)}]$$

But the total substrate concentration ($[\mathrm{S}]_\mathrm{t}$) is the sum of free substrate (S) and metal ion bound substrate (M (II) S) concentrations, respectively:

$$[\mathrm{S}]_t = [\mathrm{S}] + [\mathrm{M(II)S}] \Rightarrow [\mathrm{S}] = [\mathrm{S}]_t - [\mathrm{M(II)S}]$$

Application of equilibrium concept finally leads to an expression for [M (II) S –VHR]:

$$\Rightarrow [\mathrm{M(II)S - VHR}] = \frac{K_1 K_2\,[\mathrm{M(II)}]\,[\mathrm{S}]_t\,[\mathrm{VHR}]_t}{(1 + K_1\,[\mathrm{M(II)}] + K_1 K_2\,[\mathrm{M(II)}]\,[\mathrm{S}]_t)} \quad (2)$$

Table IV Computation of Formation Constants of [M(II)-S] Complexes from the Benesi–Hildebrand Equation $y = mx + c$; $y = [S]/d$; $x = [M(II)$

System	System	Peak (nm)	Type of Shift	Reciprocal Equation	(K_1) or (K_2)	ε	$-\Delta G$ (kJ/mol)
Binary (K_1)	Cu(II) + OHAP	402	Hypsochromic	$y = 5E-06x + 0.002$; $R^2 = 0.994$	400	500	14.84
	Ni(II) + OHAP	463	Hypsochromic	$y = 2E-0\,6x + 0.002$; $R^2 = 0.981$	1000	500	17.11
	Co(II) + OHAP	533	Bathochromic	$y = 5E-06x + 0.011$; $R^2 = 0.984$	2200	90.9	19.06
Ternary (K_2)	Cu(II) + OHAP + VHR	470	Hypsochromic	$y = 7E-7x + 0.0006$; $R^2 = 0.926$	53.5	66.7	9.86
	Ni(II) + OHAP + VHR	488, 477	Hypsochromic	$y = 1E-7x + 0.0006$; $R^2 = 0.985$	150	66.7	12.41
	Co(II) + OHAP + VHR	589, 685	Bathochromic	$y = 2E-06x + 0.001$; $R^2 = 0.986$	5.63	40.00	4.30

Using the Beer–Lambert law, the equation can be rewritten with the absorption coefficients and concentrations of each component:

$$A = \varepsilon\,[\text{M(II)S} - \text{VHR}]\;\; b$$

$$\text{(where } b = \text{path length)}$$

$$\Rightarrow [\text{M(II)S} - \text{VHR}] = A/\varepsilon\;\; b;$$

$$\text{and when } b = 1\,\text{cm}$$

$$\Rightarrow [\text{M(II)S}] = A/\varepsilon$$

Substituting [(M(II)S –VHR)] in the binding isotherm equation (2), the equilibrium constant K can now be correlated to the change in absorbance due to the formation of the [(M(II)S–VHR)] complex:

$$\Rightarrow A = \frac{(K_1K_2\,[\text{M(II)}]\,[\text{S}]_t\,[\text{VHR}]_t)}{(1 + K_1\,[\text{M(II)}] + K_1K_2\,[\text{M(II)}]\,[\text{S}]_t)}$$

$$= \frac{\varepsilon\,(K_1K_2\,[\text{M(II)}]\,[\text{S}]_t\,[\text{VHR}]_t)}{1 + K_1\,[\text{M(II)}] + (1 + K_2\,[\text{S}]_t)}$$

Reciprocals of the above equation with proper rearrangement afford

$$\frac{[\text{S}]_t\;[\text{VHR}]_t}{A} = \frac{1}{\varepsilon\,(K_1K_2\,[\text{M(II)}])} + \frac{(1 + K_2\,[\text{S}]_t)}{\varepsilon\;K_2}$$

Now from the reciprocal plot with ($[S]_t\,[VHR]_t/\Delta A$) as a function of 1/[M(II)], a straight line with$_{an}$ intercept $= (1 + K_2[S]_t)/\,\varepsilon K_2$ and slope $= 1/\varepsilon(K_1K_2)$ should be obtained. From the intercept value, ε can be computed with the assumption that ($1 \ll K_2[S]_t$), which ultimately leads to the intercept $= [S]_t\,/\varepsilon$, whereas K_2 can be calculated from the slope with proper substitution of K_1 evaluated earlier for the binary system. Representative plots are shown in Fig. 7. Free energy (ΔG) values for formation constants (K_1 and K_2) are evaluated from the vant Hoff's isotherm according to standard procedures and compiled in Table IV:

$$\Delta G = -RT\;\ln\;K_i$$

Mechanistic Scheme. On the basis of the kinetic and spectroscopic features coupled with evidence for ternary complex formation, the most plausible mechanism for metal ion–catalyzed VH reactions with acetophenone and OHAP could be proposed with the participation of the ternary precursor [M(II)-(S)(VHR)] in the rate-limiting step as shown in Schemes 2 and 3, respectively.

For Schemes 2 and 3, the rate law for the M(II)-catalyzed reaction could be given as in Eq. (3)

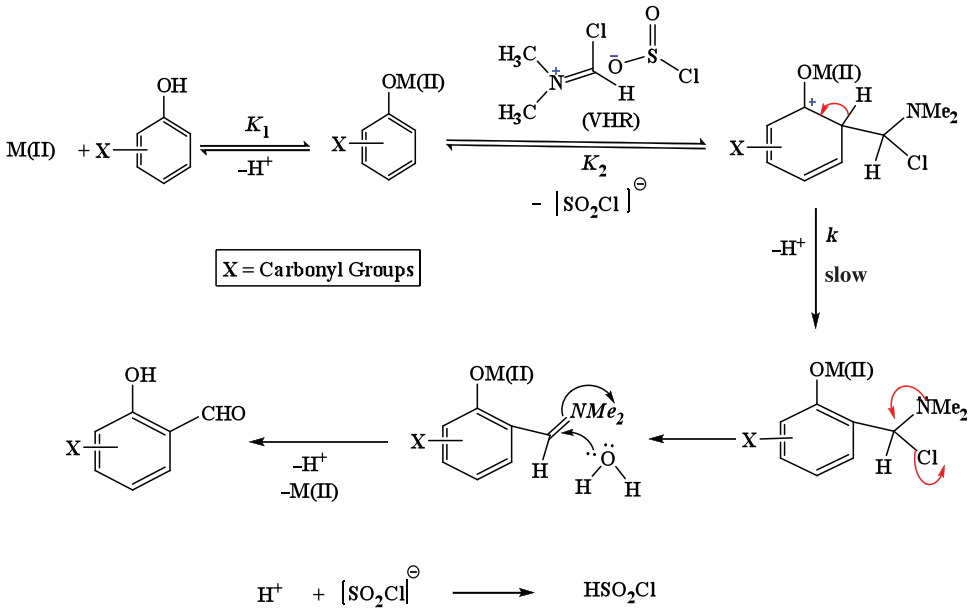

Scheme 2 Reaction mechanism for metal ion–catalyzed VH reaction with acetophenone.

on the basis of discussion given in the Supporting Information:

$$V = \frac{k_c K_1 K_2\,[\mathrm{M(II)}]\,[\mathrm{S}]_t\,[\mathrm{VHR}]_t}{1 + K_1\,[\mathrm{M(II)}]\;(1 + K_2[\mathrm{S}]_t)} \tag{3}$$

This rate law shows first-order kinetics with respect to [VHR] and fractional order in both [substrate] as well as [M(II)]. But experimental observations of the present study revealed first-order kinetics in both the reactants [VHR] and [substrate] associated with highly significant rate enhancements and yields of the products, which are clearly demonstrated in Tables I–III. This change from theory to experiment could be explained due to the small contribution of the term $(K_1K_2\ [\mathrm{M(II)}][\mathrm{S}]_t)$ in the derived rate equation. If $(1+\ K_1[\mathrm{M(II)}]) \gg K_1K_2\ [\mathrm{M(II)}][\mathrm{S}]_t$ in the denominator of the above rate equation, the contribution of $(K_1K_2[\mathrm{M(II)}][\mathrm{S}]_t)$ could be neglected. The rate equation now takes the following form:

$$V = \frac{k_c K_1 K_2\,[\mathrm{M(II)}]\,[\mathrm{S}]_t\,[\mathrm{VHR}]_t}{1 + K_1\,[\mathrm{M(II)}]}$$

Upon rearrangement, the rate law becomes

$$\frac{V}{[\mathrm{S}]_t\,[\mathrm{VHR}]_t} = k^{=}\frac{(k_c K_1 K_2\,[\mathrm{M(II)}])}{1 + K_1\,[\mathrm{M(II)}]}$$

It is reasonable to neglect contribution of $K_1[\mathrm{M(II)}] \lll 1$ in the denominator of the above equation, as [M(II)] is far less than either [S] or [VHR]. Therefore, the rate law finally takes the following form:

$$k^{=} k_c K_1 K_2\,[\mathrm{M(II)}]$$

Activation parameters are computed from Eyring's equation using the theory of reaction rates [22]. According to Eyring's theory of reaction rates, the rate constant (k) can be given as

$$k = (k_t)\,(RT/Nh)\ \exp\,(-\Delta G^{\#}/RT) \tag{4}$$

In the above equation, the transmission coefficient (k_t) is assumed to be unity, R, N, h, and T represent the gas constant, Avogadro's number, Planck's constant, and reaction temperature, and $\Delta G^{\#}$ the free energy of activation, respectively. Rearrangement of the above equation gives the following equation:

$$\exp\,(\Delta G^{\#}/RT) = (RT/Nhk) \tag{5}$$

Natural logarithm for the above equation gives

$$\Delta G^{\#} = RT\mathrm{1n}\,(RT/Nhk) \tag{6}$$

The free energy of activation ($\Delta G^{\#}$) has been obtained at various temperatures by using the above equation. An almost similar magnitude of free energies of activation ($\Delta G^{\#}$ presented in Table V) probably indicates that a similar type of mechanism is operative in both the VH systems studied irrespective of the nature of the oxychloride used for the VH reagent. Enthalpy

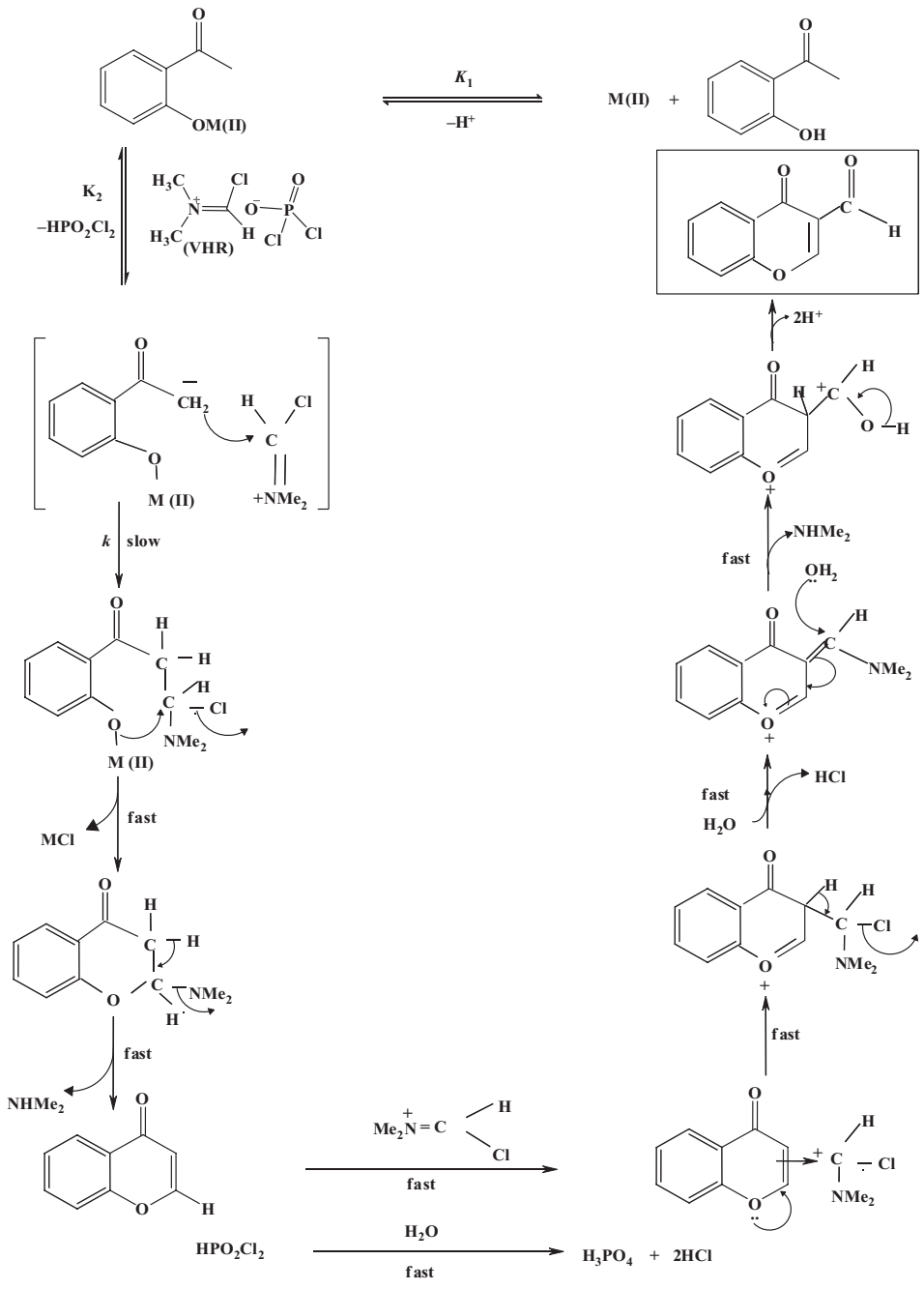

Scheme 3 Reaction mechanism for the metal ion–catalyzed VH reaction with OHAP.

($\Delta H^{\#}$) and entropy of activation ($\Delta S^{\#}$) are obtained from the plots of $\Delta G^{\#}$ as a function of temperature (T) (Fig. 8), using the Gibbs–Helmholtz equation:

$$\Delta G^{\#} = \Delta H^{\#} - T\Delta S^{\#} \qquad (7)$$

According to this equation, $\Delta G^{\#}$ as a function of temperature (T) should be linear with negative slopes of the Gibbs–Helmholtz plots gave ($\Delta S^{\#}$), whereas observed definite intercepts on the ordinate afforded ($\Delta H^{\#}$) values. Activation parameters have been evaluated for all the substrates studied in this reaction, and the data are presented in Tables V and VI. It is of interest to note that free energies of activation ($\Delta G^{\#}$) observed for DMF/$SOCl_2$ versus (DMF/$POCl_3$)VH reactions are by and large linear, indicating that a similar type of mechanism is operative. Small entropies of activation ($\Delta S^{\#}$) presented in these tables probably suggest that the transition state is tending toward de-

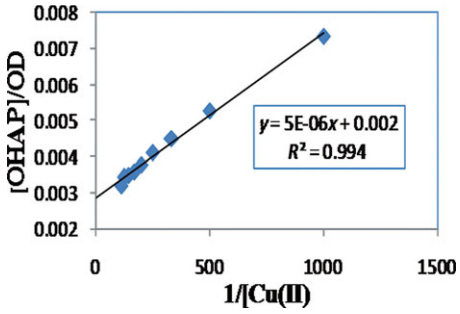

Figure 6 Benesi–Hildbrand plots for K_1.

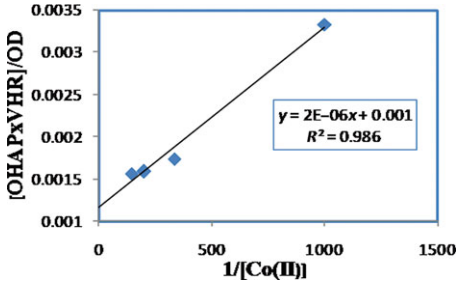

Figure 7 Reciprocal plots for K_2.

composition to yield stable products. Negative free energy values (ΔG) calculated for binding constants K_1 and K_2 (Table IV) indicate spontaneous nature of complex formation during the course of reaction.

To have a further insight into the activation parameters, we have tried to correlate ($\Delta H^{\ddagger}$) values with ($\Delta S^{\ddagger}$) obtained for both DMF/$POCl_3$ and DMF/$SOCl_2$ systems under uncatalyzed and metal ion–catalyzed systems. The plots of ($\Delta H^{\ddagger}$) values with ($\Delta S^{\ddagger}$) were linear with a positive slope and intercept. The correlation coefficients (R^2 values) obtained for these plots are in the range of a well to fairly good linear relationship (compiled in Table VII). These observations satisfy the following Leffler's equation:

$$\Delta H^{\ddagger} = \beta \Delta S^{\ddagger} + \Delta H_0^{\ddagger}$$

The slope of the Leffler's plot represents the "isokinetic temperature" ("β," the temperature (T)) at which all members of a series obeying the isokinetic relationship react at the same rate. According to Leffler's theory [26], such linearity indicates compensation of both enthalpy and entropy factors in controlling the reactions in a series of structurally related substrates

Table V Temperature-Dependent Free Energy of Activation Using Second-Order Rate Constants for VH Formylation Reactions with Acetophenones in MeCN Medium

			$\Delta G^{\#}$ (kJ/mol)				
System	Substrate	Temperature (K)	Uncatalyzed	Cu(II)	Ni(II)	Co(II)	Cd(II)
DMF/$POCl_3$	Acetophenone	313	72.16	70.38	70.60	70.78	71.65
		323	71.94	70.28	70.55	70.60	71.26
		333	71.75	70.18	70.46	70.51	71.17
	OHAP	313	71.62	70.03	70.38	70.64	70.80
		323	71.41	69.98	70.33	70.60	70.54
		333	71.17	69.92	69.90	70.38	70.48
	2,5-Dihydroxyacetophenone	313	71.62	69.92	70.26	70.50	70.78
		323	71.19	69.33	69.76	69.93	70.33
		333	70.75	68.94	69.34	69.66	69.98
	p-Nitroacetophenone	313	71.83	70.78	71.10	71.25	71.65
		323	71.66	70.72	71.05	71.19	71.42
		333	71.27	69.83	70.13	70.39	70.59
DMF/$SOCl_2$	Acetophenone	313	72.31	70.78	70.93	71.25	71.62
		323	72.24	70.60	70.72	71.05	71.58
		333	72.19	70.51	70.67	70.67	71.41
	OHAP	313	73.64	71.84	72.06	72.58	72.87
		323	73.44	71.58	71.70	72.35	72.70
		333	73.20	71.24	71.52	71.87	72.28
	2,5-Dihydroxyacetophenone	313	74.70	72.93	73.23	73.64	74.70
		323	74.45	72.59	72.98	73.46	73.9
		333	74.06	71.75	72.70	73.33	73.50
	p-Nitroacetophenone	313	73.64	71.20	71.25	71.43	73.60
		323	72.71	71.19	71.19	71.26	72.36
		333	72.19	70.90	71.14	71.05	71.56

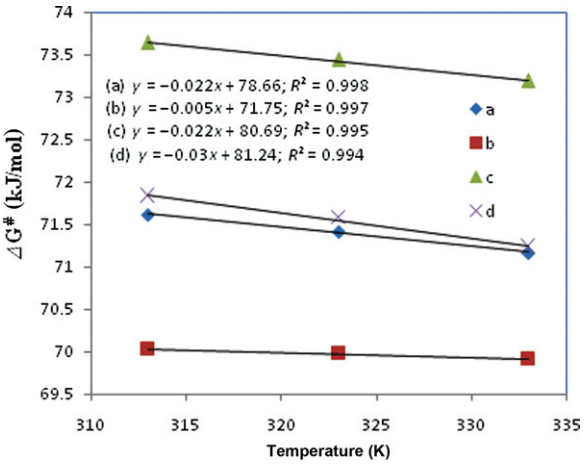

Figure 8 Gibbs–Helmholtz plots for VH formylation of orthohydroxy acetophenone at 333 K and MeCN solvent. (a) Uncatalyzed reaction using ($POCl_3$+DMF) as VH reagent. (b) Cu(II)-catalyzed reaction using ($POCl_3$+DMF) as VH reagent. (c) Uncatalyzed VH formylation of orthohydroxy acetophenone using ($SOCl_2$+DMF). (d) Cu(II)-catalyzed formylation using ($SOCl_2$+DMF).

that undergo the same change or when the reaction conditions for a single substrate are changed in a systematic way. However, the supposed isokinetic relationships as established by a direct correlation of $\Delta H^{\ddagger}$ with $\Delta S^{\ddagger}$ are often spurious and has been criticized by Exner, Peterson, Cornish-Bowden, and others [27,28]. In view of this large criticism, we can at best say that the linearity of Leffler's plots coupled with almost a similar magnitude of free energies of activation ($\Delta G^{\ddagger}$) presented in Table III indicates that a similar type of mechanism is operative in the present study.

CONCLUSIONS

In summary, we have successfully demonstrated transition metal ion–catalyzed VH formylation reactions with acetophenones in acetonitrile medium. The VH reactions followed second-order kinetics and afforded acetyl derivatives under kinetic conditions also irrespective of the nature of oxychloride used for the preparation of VH reagent along with DMF. Reactions are accelerated remarkably in the presence of transition metal ions. The present finding is advantageous for un-

Table VI Enthalpy and Entropy of Activation Parameters for VH Formylation Reactions with Acetophenones in MeCN Medium

		$\Delta H^{\#}$ (kJ/mol)					$\Delta S^{\#}$ (J/K/mol)				
System	Substrate	Uncatalyzed	Cu(II)	Ni(II)	Co(II)	Cd(II)	Uncatalyzed	Cu(II)	Ni(II)	Co(II)	Cd(II)
DMF/$POCl_3$	Acetophenone	76.9	73.4	73.3	73.8	79.4	15.0	10.0	10.0	10.0	25.0
	OHAP	79.4	71.9	78.1	76.0	77.0	25.0	6.00	24.0	17.0	20.0
	2,5-Dihydroxyacetophenone	84.9	85.5	84.3	84.5	83.2	42.0	50.0	45.0	45.0	40.0
	p-Nitroacetophenone	80.6	85.8	86.9	85.4	87.5	28.0	47.0	50.0	45.0	50.0
DMF/$SOCl_2$	Acetophenone	74.3	75.0	75.6	80.3	74.7	6.00	13.0	15.0	29.0	10.0
	OHAP	81.4	81.2	79.8	83.7	82.1	25.0	30.0	25.0	35.0	20.0
	2,5-Dihydroxyacetophenone	84.0	91.5	81.0	78.3	93.4	30.0	59.0	25.0	15.0	60.0
	p-Nitroacetophenone	97.0	75.1	73.0	75.5	106	75.0	12.0	5.00	13.0	105.0

Table VII Leffler's Plots ($\Delta H^{\#}$ vs. $\Delta S^{\#}$)

System	System	Equation	β (K)
DMF/$POCl_3$	Uncatalyzed	$y = 0.299x + 72.22$; $R^2 = 0.995$	299
	Cu(II)	$y = 0.320x + 70.10$; $R^2 = 0.995$	320
	Ni(II)	$y = 0.328x + 70.05$; $R^2 = 0.995$	328
	Co(II)	$y = 0.318x + 70.59$; $R^2 = 0.996$	318
	Cd(II)	$y = 0.331x + 70.59$; $R^2 = 0.986$	331
DMF/$SOCl_2$	Uncatalyzed	$y = 0.323x + 73.18$; $R^2 = 0.992$	323
	Cu(II)	$y = 0.353x + 70.62$; $R^2 = 0.999$	353
	Ni(II)	$y = 0.380x + 70.7$; $R^2 = 0.961$	380
	Co(II)	$y = 0.304x + 72.44$; $R^2 = 0.954$	304
	Cd(II)	$y = 0.312x + 73.79$; $R^2 = 0.981$	312

derstanding the nature of reactive species as well as the mechanism of acetylation.

BIBLIOGRAPHY

1. Nawrot-Modranka, J.; Nawrot, E.; Graczyk, J. Eur J Med Chem 2006, 41, 1301.
2. Horton, D. A.; Bourne, G. T.; Smythe, M. L. Chem Rev 2003, 103, 893.
3. Sabitha, G. Aldrichim Acta 1996, 29, 15.
4. Wang, B.; Yang, Z. Y.; Li, T. Bioorg Med Chem 2006, 14, 6012.
5. Kawase, M.; Tanaka, T.; Kan, H.; Tani, S.; Nakashima, H.; Sakagami, H. In Vivo 2007, 21, 829.
6. Shrestha, S.; Hwang, S.Y.; Lee, K. H.; Cho, H. Bull Korean Chem Soc 2005, 26, 1138.
7. Lacova, M.; Loos, D.; Furdik, M.; El-Shaaer, H. M.; Matulova, M. In First International Electronic Conference on Synthetic Organic Chemistry (ECSOC-1). Available at www.mdpi.org/ecsoc/. Accessed September 1997.
8. (a) Vilsmeier, A.; Haack, A. Ber 1927, 60, 119; (b) Meth, S. P.; Cohn, O.; Stanforth, S. P. Comp Org Synth 1991, 2, 777; (c) Campaigne, E.; Archer, W. L. Org Synth Coll 1963, 4, 331; 1953, 33, 27; (d) Arnold, Z.; Holy, A. Collect Czech Chem Commun 1962, 27, 2886.
9. (a) Arnold, Z.; Holy, A. Collection Czech Chem Commun 1962, 27, 2886; (b) Smith, T. D. J. Chem Soc A 1966, 841; (c) Lieoscher, H. Collect Czech Chem Commun 1976, 41, 1565; (d) Anderson, A. G.; Owen, N. E. T.; Franon, F. J.; Ereckson, D. Synthesis 1966, 398.
10. (a) Martin, G. J.; Poignant, S.; Filleux, M. L. Quemeneeuer, M. T. Tetrahedron Lett 1970, 58, 5061; (b) Martin, G.; Martin, M. Bull Soc Chem Fr 1963, 1637; (c) Martin, G. J.; Poignant, S. J Chem Soc, Perkin Trans 2 1972, 1964; 1974, 642.
11. (a) Lorenz, A.; Winzinger, R. Helv Chem Acta 1945, 28, 600; (b) Boshard, H. H.; Zollinger, H. Helv Chem Acta 1959, 42, 1659.
12. (a) Alumi, S.; Linda, P.; Marino, G.; Santine, S.; Salvelli, G. J Chem Soc, Perkin Trans 2 1972, 2070; (b) Linda, P.; Lucccarelli, A.; Marino, G.; Savelli, G. J Chem Soc, Perkin Trans 2 1974, 1610.
13. Ali, M. M.; Tasneem Rajanna, K. C.; Saiprakash, P. K. Synlett 2001, 251.
14. Ali, M. M.; Sana, S.; Tasneem Rajanna, K. C.; Saiprakash, P. K. Synth Commun 2002, 32, 1351.
15. (a) Chakradhar, A.; Roopa, R.; Rajanna, K. C.; Saiprakash, P. K. Synth Commun 2009, 39; (b) Rajanna, K. C.; Satish Kumar, M.; Venkanna, P.; Ramgopal, S.; Venkateswarlu, M. Int Natl J Org Chem 2011, 1, 250; (c) Venkateswarlu, M.; Rajanna, K. C.; Satish Kumar, M.; Umesh Kumar, U.; Ramgopal, S.; Saiprakash, P. K. Int Natl J Org Chem 2011, 1, 233; (d) Satish Kumar, M.; Venkanna, P.; Ramgopal, S.; Ramesh, K.; Venkateswarlu, M.; Rajanna, K. C. Organic Commun 2012, 5, 42.
16. Ali, M. M. Doctoral thesis, Osmania University: Hyderabad, India, 2002.
17. Rajanna, K. C.; Soloman, F.; Ali, M. M.; Saiprakash, P. K. Tetrahedron 1996, 52, 3669.
18. (a) Rajanna, K. C.; Soloman, F.; Ali, M. M.; Saiprakash, P. K. Int J Chem Kinet 1996, 28, 865; (b) Rajanna, K. C.; Venkateswarlu, M.; Satish Kumar, M.; Umesh Kumar, U.; Ramgopal, S.; Saiprakash, P. K. Helv Chim Acta 2011, 94, 2168; (c) Rajanna, K. C.; Venkateswarlu, M.; Satish Kumar, M.; Umesh Kumar, U.; Venkateshwarlu, G.; Saiprakash, P. K. Int J Chem Kinet 2013, 45, 69.
19. Nohara, A.; Umetani, T.; Sanno, Y. Tetrahedron 1974, 30, 3553.
20. (a) Nohara, A.; Umetani, T.; Sanno, Y. Tetrahedron Lett 1973, 14, 1995; (b) Su, W. W.; Li, Z. H.; Zhao, L. Y. Org Prep Proc Int 2007, 39, 495.
21. Thompson, D. T. Coord Chem Rev 1996, 154, 179.
22. Jagirdar, B. R. Resonance 1999, 63.
23. Hegedus, L. S. Coord Chem Rev 2004, 204, 199.
24. (a) Benesi, H.; Hildebrand, J. J Am Chem Soc 1949, 71, 2703; (b) Rao, C. N. R. Ultraviolet and Visible Spectroscopy; Butterworths: London, 1961; (c) Ketelaar, J. A. A.; von de Stolpe, C.; Goud-Smit, A.; Dzubas, W. Rec Trav Chim. 1952, 71, 1104.
25. (a) Laidler, K. J. Chemical Kinetics, 3rd ed.; Harper and Row: New York, 1987; (b) Laidler, K. J.; Meiser, J. H. Physical Chemistry, 3rd ed.; Houghton Mifflin: New York, 1999.
26. Leffler, J. J Org Chem 1955, 20, 1202.
27. (a) Petersen, J. R. C. J Org Chem 1964, 29, 3133; (b) Exner, O. Nature 1964, 201, 488; Prog Phys Org Chem 1973, 10, 411.
28. (a) Liu, L.; Guo, Q. X. Chem Rev 2001, 101, 673; (b) Cornish-Bowden, A. J Biosci 2002, 27, 121.